

## P2.15 PLUMES ABOVE THUNDERSTORM ANVILS AND THEIR CONTRIBUTIONS TO CROSS TROPOPAUSE TRANSPORT OF WATER VAPOR IN MIDLATITUDES

Pao K. Wang\*

Department of Atmospheric and Oceanic Sciences  
University of Wisconsin-Madison  
Madison, WI

### 1. INTRODUCTION

Water vapor is important to the radiative budget to the atmosphere, and hence to climate studies, because of its strong absorption of infrared (IR) radiation (e.g., Liou, 1984; Goody and Yung, 1989). It is also the main source of ozone-destroying HO<sub>x</sub> radicals in the lower stratosphere. In the condensed phase, as exemplified by the recently observed anvil-top plumes (Setvak and Doswell, 1991; Levizzani and Setvak, 1996) to be discussed in detail later, it serves as a catalytic surface for heterogeneous reactions involving NO<sub>x</sub> and halogen species (e.g., Solomon, 1999). It is clear that the distribution of water substance in the upper troposphere/lower stratosphere (UT/LS) region has significant impacts on the global climate process.

In order to assess the impact of water vapor, we need to understand how it is transported in the stratosphere. At present, the global scale transport of water vapor in the lower stratosphere is thought to be due to the *extratropical pumping* mechanism generated by breaking Rossby waves and related potential-vorticity-transporting motions in the midlatitude atmosphere (Holton et al., 1995). In this scenario, the main source of lower stratospheric water vapor is the deep tropical convective clouds that pump water vapor from the troposphere to the stratosphere. Oxidation of methane may represent a minor water vapor source in the lower stratosphere. The tropical stratospheric water vapor is then transported poleward by the midlatitude "pumps" so that the middle and higher latitudes are basically a water vapor sink. However, recent observations suggest that this simple mechanism may be inadequate for explaining finer details of the water vapor transport. For example, aircraft measurements done by Foot (1984) over 45–65°N indicated that the midlatitude lower-stratospheric water vapor

concentration is much higher than can be explained solely by tropical entry of air. There are also seasonal and hemispheric variations of lower-stratospheric water vapor that cannot be explained by the mean circulation scenario alone. Also, results of ER-2 research aircrafts measurements during the Airborne Antarctic Ozone Experiment (AAOE) and the Airborne Arctic Stratospheric Expedition (AASE) showed that the wintertime water vapor fields in the lower stratosphere display a hemispheric asymmetry, with much lower early spring values in the southern hemisphere (SH) than the northern hemispheric (NH) (Kelly et al., 1990). Export of dehydrated air from the polar vortex was investigated as the possible mechanism for the asymmetry.

Using water vapor data from the Stratospheric Photochemistry, Aerosols and Dynamics Expedition (SPADE), Hintsa et al. (1994) found higher water vapor concentration in the NH in fall than in spring. Further analyses of water vapor profile measurements during SPADE (Dessler et al., 1995) show that water vapor mixing ratios in the lowermost stratosphere are consistent with a significant influx of air into the lowermost stratosphere from the extratropical upper troposphere. Pan et al. (1997), using Stratospheric Aerosol and Gas Experiment II (SAGE II) data, found a strong seasonal cycle of the water vapor mixing ratio on the 320-K isentropic surface for both hemispheres, with maximum values in summer and minimum values in early spring. By also analyzing SAGE II ozone data, they inferred from both water vapor and ozone data that extratropical UT/LS exchange has a significant influence on the lowermost stratosphere, especially in the NH summer season.

### 2. SATELLITE OBSERVATIONS OF PLUMES ABOVE THUNDERSTORM ANVILS

\* Corresponding author address: Pao K. Wang  
Department of Atmospheric and Oceanic Sciences  
University of Wisconsin-Madison  
Madison, WI 53706. Email: Pao@windy.meteor.wisc.edu

The observations mentioned in the preceding section are mainly concerned with stratospheric water vapor measurements but do not pinpoint its possible transport mechanisms. A few other observations, on the other hand, provide some clues. Roach (1967) and Fujita (1982) pointed out observations of cirrus clouds atop the anvils of some severe thunderstorms, and mentioned that they were produced by collapsing overshooting tops, although the source of water vapor was not clear. More recently, Setvak and Doswell (1991) and Levizzani and Setvak (1996) reported the observation of plume-like features on top of some convective storms in Advanced Very High Resolution Radiometer (AVHRR) satellite imagery of the US National Oceanographic and Atmospheric Administration (NOAA) polar orbiters. Examples of the anvil-top plumes are shown in Fig. 1. These studies were based on the AVHRR channels 2 (0.625-1.1  $\mu\text{m}$ ), 3 (3.55-3.93  $\mu\text{m}$ ), and 4 (10.3-11.3  $\mu\text{m}$ ) but some visible characteristics in channel 1 (visible) are also included. Some of the major characteristics listed below, based on Levizzani and Setvak (1996), are common to all plumes whereas others hold only in specific cases:

- (a) A small bright spot in channel 2 a few pixels across, i.e., a few kilometers, in the form of an oval cloud, is detected as the plume's source. The shadow cast by this rounded cloud appears much longer than that of the plume, suggesting a higher altitude. The source spot is normally shifted downwind from the coldest area, and collocated with the storm's embedded warm area.
- (b) These cloud plumes spread downwind, resembling smoke plumes from a chimney. The estimated height in one case is about 15 km.
- (c) They are vertically separated from the underlying anvils, as deduced from the shadows they cast on the anvils.
- (d) Plumes are partially transparent in channels 1 and 2, and one can often see through them and discern some features on the underlying anvil. This indicates that the plumes are usually very thin and tenuous.
- (e) The structure of the plume is more or less preserved in channel 4, indicating a temperature difference between the particles of the plume and the surroundings.
- (f) Sometimes the plume splits into two very bright splinters with a cyclonically curved northern branch and *anticyclonic* southern branch. The source of the split plume appears to be in the distant warm area.

It is the purpose of this paper to show that the plume formation is closely linked to the strong updraft and overshooting of a severe thunderstorm. The requisite water vapor comes from the storm below, hence representing a transport of water vapor from the troposphere to the lower stratosphere. This conclusion is achieved by using a three-dimensional (3D) numerical cloud model capable of simulating the

evolution of major dynamical and microphysical processes in a deep convective storm. Careful analysis of the simulation results reveals cloud features strikingly similar to the aforementioned plume characteristics as reported by Levizzani and Setvak (1996).

### 3. DESCRIPTION OF THE CLOUD MODEL WISCDYMM

The cloud model utilized for the present study is the Wisconsin Dynamical/Microphysical Model (WISCDYMM), which is a 3D quasi-compressible, time-dependent, non-hydrostatic cloud model developed at the University of Wisconsin-Madison by the author's group. The governing equations and microphysical parameters are given in Straka (1989) and Johnson et al. (1994).

### 4. THE 2 AUG 1981 CCOPE SUPERCELL

The simulated storm for illustrating the plume-formation mechanism is a supercell that passed through the center of the Cooperative Convective Precipitation Experiment (CCOPE) (Knight, 1982) observational network in southeastern Montana on 2 August 1981. The storm and its environment were intensively observed for more than 5 h by a combination of seven Doppler radars, seven research aircraft, six rawinsonde stations and 123 surface recording stations as it moved east-southeastward across the CCOPE network. This storm case was chosen because it provides much detailed observational data for comparison with model results in dynamics and cloud physics, and the author's group has obtained successful simulations of it previously.

### 5. RESULTS AND DISCUSSIONS

Simulations were performed using three different resolutions:  $1 \times 1 \times 0.5 \text{ km}^3$ ,  $1 \times 1 \times 0.2 \text{ km}^3$ , and  $0.5 \times 0.5 \times 0.2 \text{ km}^3$ . All three simulations show the plume phenomenon well in that they all exhibit similar plume characteristics. The overall features for the latter two grids are quite similar, except that the one with refined horizontal resolution shows more detailed midlevel horizontal structure than the other two runs. Since the utmost concern in this study is the vertical transport, it was decided to choose the simulation results with the refined vertical resolution ( $1 \times 1 \times 0.2 \text{ km}$ ) for analysis here. The overall dynamical and microphysical characteristics of the new results, being very similar to those reported by Johnson et al. (1994), will not be discussed here.

The original 1746 MDT Knowlton, Montana sounding did not contain moisture information above 300 mb. The simulation of Johnson et al. (1994) was performed under the assumption of no water vapor above 300 mb initially (hereafter called the "dry-

case"). But since the present study is concerned with water vapor transport, this assumption may be inappropriate. To ensure that the upper level (above 300 mb) moisture is properly represented, two additional options modifying the upper level dewpoint profile were made and tested: (1) using an average August 1999 Halogen Occultation Experiment (HALOE) water vapor profile over midlatitudes ( $40^{\circ}$ - $60^{\circ}$ N) to represent the upper level humidity, (2) shifting the upper level  $T_d$  profile of option 1 to the right so that the 300 mb level is exactly saturated with respect to liquid water (not shown). The simulation results with option 2 do not show clear plume structure and therefore will not be considered further. The results of option 1 do not differ significantly from the dry case.

### *Central Cross-section Features*

Figure 1 shows a series of snapshots of the vertical profiles of *relative humidity with respect to ice*, RHi, in the central west-east cross-section ( $y = 27$  km) where the storm activity is usually the most vigorous. The reason to use RHi profiles rather than RHw, the relative humidity with respect to liquid water, is that ice formation is more relevant in the cloud top due to the prevailing cold temperatures there. Note that only the portion of the storm above 10 km is shown in each panel. A comparison between the water vapor mixing ratio  $q_v$  and RHi profiles shows that the two are very similar. Hence the RHi profile can be viewed as essentially the same as the  $q_v$  profile. The range in Fig. 4 are windowed to 10-20 km vertically and 20-55 km horizontally, with the vertical scale stretched by ~35% in these views.

No obvious plume structure is discernible before 20 min into the simulated storm activity. At 24 min, strong gravity wave motions at the cloud top are visible. There is a large surge of high humidity region above the second wave crest (to the east of the main updraft column) that seems to propagate upward and westward (i.e., towards upstream relative to the upper level wind direction) into the stratosphere. At 32 min, this moist surge appears to be nearly detached from the anvil of the storm and forms a separate moist layer in the stratosphere. At 36 min, the surge appears to break into two parts; the one to the west seems to merge with the uprising overshooting dome, while the one to the east seems to form a separate plume-like structure. This latter plume, sloping downward almost parallel to the slope of the anvil, appears to gradually dissipate with time into much more diffuse moist layer. This surge mechanism may be responsible for the formation of the stratospheric cirrus as observed by Fujita (1982), who stated that "One of the most striking features seen repeatedly above the anvil top is the formation of cirrus cloud which jumps upward from behind the overshooting dome as it collapses violently into the anvil cloud". Some more details of this phenomenon will be examined in the next section. While this mechanism may form some cirrus in the stratosphere, it does not

seem to produce the main plumes as seen in the satellite images. However, it may be responsible for the formation of plumes in the "distant warm area" as described in Point (f) in Sec. 2.

At 48 min, a "blob" of moist air appears on top of the overshooting dome of the storm. The size of this blob fluctuates at first, but it eventually becomes larger and, beginning at 80 min, it gradually takes on the shape of a chimney plume, much as described in Sec. 2. The stretching of the plume downwind is apparently caused by the upper-level winds, which are predominantly westerly. The maximum RHi humidity in the core of the plume sometimes exceeds 100%. At 112 min, the plume has reached the east boundary of the computational domain. Its altitude is between 15 and 16 km, roughly the same as that observed by Levizzani and Setvak (1996). The plume associated with the gravity wave crest, on the other hand, is located at 12 - 13 km. Thus there may be more than one layer of plumes at a given time. The thickness of the plumes depends on the choice of critical RHi for defining their boundaries. If we use 90% RHi, then the thickness can range from several hundred meters to about 1 km. A choice of smaller critical RHi will naturally lead to a somewhat thicker plume layer. Judging from the extremely small amount of water vapor mixing ratio in the plume, any condensed water would also have extremely small concentrations and hence be semi-transparent. It is also clear from the pictures that there is a shallow dry layer immediately above the anvil. This dry layer is about 1 ~ 1.5 km thick and apparently extends to the whole length of the anvil in the computational domain.

### *Other notable cloud top features*

There are other notable cloud top features related to the plume phenomenon and they will be reported during the conference. The possible mechanism responsible for plume formation will also be discussed at that time.

**Acknowledgments.** I am grateful to Susan Solomon for pointing out relevant references and for her encouraging and helpful comments, to Liwen Pan for sharing the SAGE II data, to Hsin-mu Lin and Yulien Chu for helping processing the model data, and to Robert Schlesinger and David Martin for many helpful comments. This study was first inspired by a discussion with Vincenzo Levizzani and Martin Setvak. This work is partially supported by NSF Grants ATM-9907761 ATM-9633424, and NASA Grant NAG5-7605.

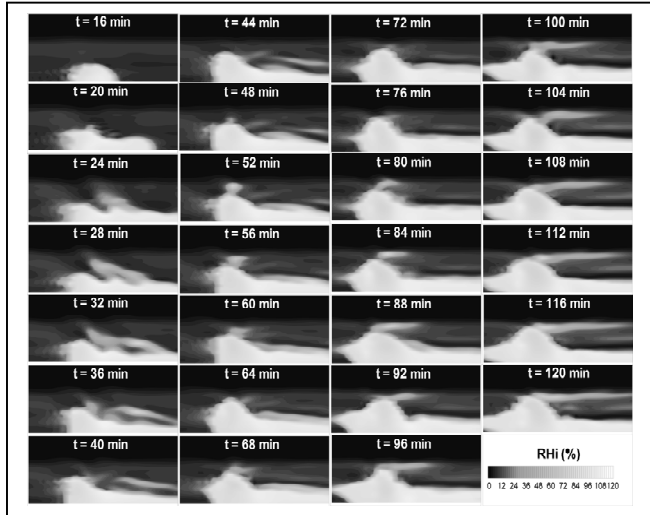


Fig. 1. Snapshots of vertical RHi (relative humidity with respect to ice) profiles every 4 min in the central east-west cross-section ( $y = 27$  km), showing the plume feature above the anvil. The vertical axis range is 10-20 km and horizontal axis range 20-55 km.

## REFERENCES

- Foot, J. S., 1984: Aircraft measurements of the humidity in the lower stratosphere from 1977 to 1980 between 45N and 65N, *Q. J. Royal Meteor. Soc.*, 110, 303-319..
- Fujita, T. T., 1982: Principle of stereographic height computations and their application to stratospheric cirrus over severe thunderstorms, *J. Meteor. Soc. Japan.*, 60, 355-368.
- Goody, R. M., and Y. L. Yung, 1989: *Atmospheric Radiation: Theoretical Basis*. Oxford University Press.
- Hintsa, E. J., E. M. Weinstock, A. E. Dessler, J. G. Anderson, M. Loewenstein, and J. R. Podolske, 1994: SPADE H<sub>2</sub>O measurements and the seasonal cycle of stratospheric water vapor, *Geophys. Res. Lett.*, 21, 2559-2562, 1994.
- Holton, J. R., P. H. Haynes, M. E. McIntyre, A. R. Douglass, R. B. Rood, and L. Pfister, 1995: Stratospheric-tropospheric exchange, *Rev. Geophys.*, 33, 403-439.
- Johnson, D. E., and P. K. Wang, and J. M. Straka, 1994: A study of microphysical processes in the 2 August 1981 CCOPE supercell storm, *Atmos. Res.* 33, 93-123.
- Kelly, K. K., A. F. Tuck, L. E. Heidt, M. Loewenstein, J. R. Podolske, S. E. Strahan, and J. F. Vedder, 1990: A comparison of ER-2 measurements of stratospheric water vapor between the 1987 Antarctic and 1989 Arctic Airborne Missions, *Geophys. Res. Lett.*, 17, 465-468.
- Knight, C. A., Ed., 1982: The Cooperative Convective Precipitation Experiment (CCOPE), 18 May-7 August 1981, *Bull. Amer. Meteor. Soc.*, 63, 386-398.
- Levizzani, V., and M. Setvak, 1996: Multispectral, high resolution satellite observations of plumes on top of convective storms, *J. Atmos. Sci.*, 53, 361-369.
- Liou, K.N., 1992: *Radiation and Cloud Processes in the Atmosphere: Theory, Observation, and Modeling*. Oxford University Press, New York, 487 pp.
- Pan, L., S. Solomon, W. Randel, J-F. Larmarque, P. Hess, J. Gille, E. Chiou, and M. P. McCormick, 1997: Hemispheric symmetries and seasonal variations of the lowermost stratospheric water vapor and ozone derived from SAGE II data, *J. Geophys. Res.*, 102, 28177-28184.
- Pan, L. L., E. J. Hintsa, E. M. Stone, E. M. Weinstock, and W. J. Randel, 2000: The seasonal cycle of water vapor and saturation vapor mixing ratio in the extratropical lowest stratosphere, *J. Geophys. Res.*, 105, 26519-26530.
- Roach, W. T., 1967: On the nature of the summit areas of severe storms in Oklahoma, *Q. J. Royal Meteor. Soc.*, 93, 318-336.
- Setvak, M. and C. A. Doswell III, 1991: The AVHRR channel 3 cloud top reflectivity of convective storms, *Mon. Wea. Rev.*, 119, 841-847.
- Solomon, S., 1999: Stratospheric ozone depletion: A review of concept and history, *Rev. Geophys.*, 37, 275-316.
- Straka, J. M., 1989: *Hail growth in a highly glaciated central high plains multi-cellular hailstorm*. Ph.D thesis, University of Wisconsin-Madison, 413pp.